

# Making Earth Science Data Records for Use in Research Environments (MEaSUREs)

## README Document for

### TOMSN7SO2

Goddard Earth Sciences Data and Information Services Center (GES DISC) <http://disc.gsfc.nasa.gov>

NASA Goddard Space Flight Center, Greenbelt, MD 20771 USA

Principal Investigators: Nickolay A. Krotkov, Pawan K. Bhartia, Code 614  
[Nickolay.A.Krotkov@nasa.gov](mailto:Nickolay.A.Krotkov@nasa.gov)  
301-614-5553

Algorithm Developer: Brad Fisher , SSAI, Code 614  
[bradford.fisher@ssaihq.com](mailto:bradford.fisher@ssaihq.com)  
301-867-2188

Algorithm Support: Peter Leonard, ADNET, Code 619  
[peter.j.leonard@nasa.gov](mailto:peter.j.leonard@nasa.gov)

**Last Revised: June 21 2019**

**Reviewed by: *Andrey Savtchenko***

Name

GES DISC

GSFC Code 610.2

Date

**Goddard Space Flight Center**

**Greenbelt, Maryland**

Name

External Organization

# Revision History

---

<i>Revision Date</i>	<i>Changes</i>	<i>Author</i>
6/26/2019	reviewed	Nickolay Krotkov
6/22/2019	reviewed	Peter Leonard
6/21/2019	Updates reflecting Version 3 improvements including: <ul style="list-style-type: none"><li>- Improvements in step 2 algorithm</li><li>- Improvements in file format to make the TOMSN7SO2 product files work better with Panoply</li></ul>	Brad Fisher

# **Table of Contents**

<b>1. INTRODUCTION.....</b>	<b>5</b>
<b>1.1 TOMS Nimbus-7 MEaSURES SO<sub>2</sub> Dataset: TOMSN7SO2 .....</b>	<b>5</b>
<b>1.2 TOMS Instrument .....</b>	<b>5</b>
<b>1.3 Science Background .....</b>	<b>7</b>
<b>2. MULTI-SATELLITE SO<sub>2</sub> ALGORITHM.....</b>	<b>8</b>
<b>2.1 General Description.....</b>	<b>8</b>
<b>2.2 Step 1 Retrieval.....</b>	<b>9</b>
<b>2.3 Step 2 Retrieval.....</b>	<b>11</b>
2.3.1 FOV Selection Criterium .....	12
2.3.2 Interpolation methodology .....	13
2.3.3 O <sub>3</sub> and SO <sub>2</sub> corrections.....	15
<b>2.4 Soft Calibration of the 340 Channel.....</b>	<b>17</b>
<b>2.5 SO<sub>2</sub> retrieval noise.....</b>	<b>19</b>
<b>3. DATASET ORGANIZATION.....</b>	<b>24</b>
<b>3.1 File Naming Convention .....</b>	<b>24</b>
<b>3.2 File Format and Structure.....</b>	<b>24</b>
<b>3.3 Key Science Data Fields .....</b>	<b>25</b>
3.3.1 SO <sub>2</sub> Column Amount .....	25
3.3.2 O <sub>3</sub> Column Amount.....	25
3.3.3 Lambertian Equivalent Reflectivity at 380 nm .....	26
3.3.4 Reflectivity Spectral Dependence ( $\partial R/\partial \lambda$ ).....	26
<b>4. DATA CONTENTS.....</b>	<b>26</b>
<b>4.1 Global Attributes .....</b>	<b>27</b>
<b>4.2 Dimensions .....</b>	<b>28</b>
<b>4.3 Data Fields.....</b>	<b>29</b>
4.3.1 Ancillary Data .....	29
4.3.2 Geolocation Data.....	29
4.3.3 Science Data.....	30
4.3.4 Sensor Data .....	31
<b>5. CONTACTS.....</b>	<b>31</b>
<b>6. REFERENCES .....</b>	<b>32</b>

## 1. INTRODUCTION

### *1.1 TOMS Nimbus-7 MEaSUREs SO<sub>2</sub> Dataset: TOMSN7SO2*

This document contains a brief description of the TOMSN7SO2 data product. TOMSN7SO2 is a Level 2, orbital track volcanic sulfur dioxide (SO<sub>2</sub>) product for the Total Ozone Mapping Spectrometer (TOMS) onboard NASA's Nimbus 7 satellite, which was launched on October 24, 1978 into polar sun-synchronous orbit and collected data from November 1, 1978 to May 6, 1993. This was the first mission to provide daily contiguous global maps of total ozone (O<sub>3</sub>). As part of the NASA's Making Earth System Data Records for Use in Research Environments (MEaSUREs) program, the Goddard Earth Science (GES) Data and Information Data Center (DISC) has released a new SO<sub>2</sub> Earth System Data Record (ESDR), TOMSN7SO2, re-processed using new 4 UV wavelength bands MS\_SO2 algorithm that spans the full Nimbus 7 data period. TOMSN7SO2 is a Level 2 orbital swath product, which will be used to study the fifteen-year SO<sub>2</sub> record from the Nimbus-7 TOMS and to expand the historical database of known volcanic eruptions.

### *1.2 TOMS Instrument*

TOMS is a fixed-grating Ebert-Fastie monochromator with photomultiplier tube detector that measures solar backscattered ultraviolet (BUV) radiances (I) at 6

narrow wavelengths bands (Full Width at Half Maximum band width  $\sim 1.1$  nm) in the near ultraviolet (UV) spectral region as well as the incident solar irradiances (F) (Heath, *et al.*, 1975). The ratio of radiance to irradiance provides the spectral reflectivity parameter used in the ozone retrieval. The wavelength band centers shown in Table 1 were selected to optimize column ozone retrievals assuming that two pairs of shorter, absorbing wavelengths would be needed to cover the full dynamic range of ozone and solar zenith angles encountered globally, similar to the Dobson Spectrophotometer design. Two additional non-absorbing longer UV-A wavelengths were provided to measure the surface or cloud reflectivity (R) and its spectral dependence.

Table 1

Channel Number	Wavelength, vacuum [nm]	Used in SO <sub>2</sub> retrieval	MS_SO2 Retrieved Parameter
1	312.34	Not Used	
2	317.35	x	SO <sub>2</sub>
3	331.06	x	O <sub>3</sub>
4	339.66	x	dR/dλ
5	359.99	Not Used	
6	379.89	x	R

TOMS scans in the cross-track direction in 3° steps from 51° on west side of nadir to 51° on the east, for a total of 35 cross-track samples. The instantaneous field-of-view (FOV) of 3° x 3° results in a footprint varying from a 50 km x 50 km approximately square FOV at nadir to a 125 km by 280 km diamond-shaped FOV at the scan extremes. The total swath width is 3000 km covering Earth's surface in 14 orbits per day.

### *1.3 Science Background*

The original design of the TOMS instrument assumed that ozone was the only significant gaseous absorber in near UV wavelengths (Dave and Mateer 1967). A second absorber was later discovered in 1982 as a high ozone anomaly observed over the El Chichon volcano in Mexico and recognized as SO<sub>2</sub> gas absorption in the volcanic cloud (Krueger 1983). Following the discovery, Krueger *et al.* (1995) developed a first algorithm to separate the ozone and SO<sub>2</sub> signals and to retrieve the column amount of SO<sub>2</sub>. The off-line retrieval has been used on a case-by-case basis to retrieve SO<sub>2</sub> mass from explosive eruptions using TOMS measurements on Nimbus-7 and follow-up missions (Krueger *et al.*, 2000; Carn *et al.*, 2003). The TOMSN7SO2 data product is the first public release of the complete Nimbus-7 TOMS SO<sub>2</sub> Level 2 data, re-processed with a new 4 UV wavelengths algorithm that is fast enough to permit production of the entire global dataset.

## 2. MULTI-SATELLITE SO<sub>2</sub> ALGORITHM

### 2.1 General Description

This section describes the new Multi-Satellite SO<sub>2</sub> (MS\_SO2) [Fisher et al., 2019]. This algorithm builds on the heritage of the TOMS total ozone (TO3) algorithm (Dave and Mateer, 1967, McPeters *et al.*, 1996), but adds sulfur dioxide (SO<sub>2</sub>) as a second absorber to the pre-computed BUUV look-up tables. The retrieval uses four of the six available spectral bands to retrieve a state vector ( $\hat{X}$ ) with 4 parameters: SO<sub>2</sub> column amount, O<sub>3</sub> column amount, the Lambertian equivalent reflectivity (LER) at 380 nm, R, and the spectral dependence of R, dR/dλ. The algorithm relies on spectral differences in SO<sub>2</sub> and O<sub>3</sub> cross sections to simultaneously quantify the amounts of the two trace gases (see Table 1 and Figure 1). SO<sub>2</sub> is more absorbing than O<sub>3</sub> at the shorter channels (312 and 317 nm), whereas O<sub>3</sub> is more absorbing at the longer absorbing channel (331 nm). Figure 1 shows the O<sub>3</sub> and SO<sub>2</sub> spectral cross sections in the near-UV spectral range and the SO<sub>2</sub> to O<sub>3</sub> cross section ratio over the same range. It is the relative difference in the cross-section ratio at 317nm and 331nm that allows for the separation of the two gases. The three vertical bars show the centers of the absorbing spectral bands used in the retrieval.

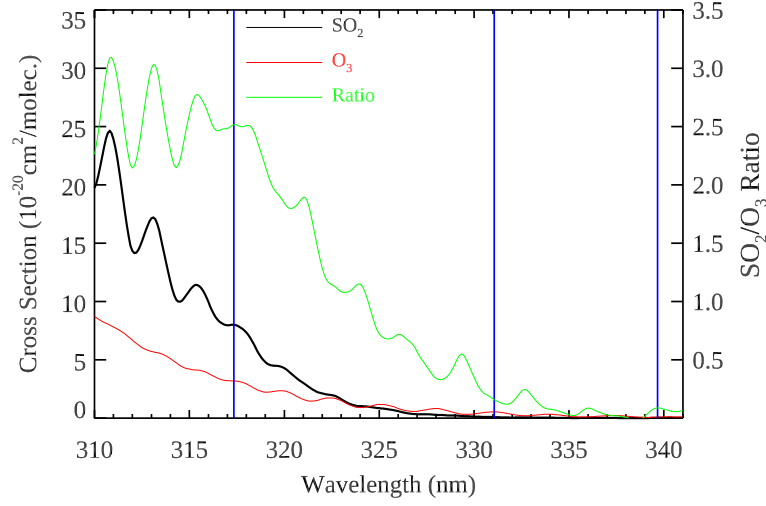


Figure 1. SO<sub>2</sub> (black) and O<sub>3</sub> (red) cross-sections and their ratio (green) at UV wavelengths. The three vertical bars show the location of the absorbing channels used in the retrieval.

## 2.2 Step 1 Retrieval

The SO<sub>2</sub> retrieval is performed in two steps and applied iteratively for each FOV. The retrieval starts with a first guess value of total column ozone based on climatology and assuming zero SO<sub>2</sub>. The LER is then computed at 380 nm (R). Because O<sub>3</sub> and SO<sub>2</sub> absorption is very weak at this wavelength, R remains fixed during the iterations. The algorithm then uses 3 shorter spectral bands to retrieve  $\Delta(\partial R/\partial \lambda)$ ,  $\Delta O_3$  and  $\Delta SO_2$  adjustments to the state vector:  $\Delta \mathbf{x} = [\Delta SO_2, \Delta O_3, \Delta(\partial R/\partial \lambda)]$ , assuming a linear  $R(\lambda)$  spectral dependence:

$$\Delta y_i = N_{m_i} - N_{c_i} = \frac{\partial N_{c_i}}{\partial SO_2} \Delta SO_2 + \frac{\partial N_{c_i}}{\partial O_3} \Delta O_3 + \frac{\partial N_{c_i}}{\partial R} (\lambda_i - \lambda_R) \Delta \frac{\partial R}{\partial \lambda} \quad (1)$$

where  $i = 1, 2, 3$  corresponds to the 317, 331, and 340nm bands and  $\lambda_R=380\text{m}$ . The left-hand side of Eq. 1 represents the difference (residual) between the measured and calculated sun normalized BUV radiances expressed in N-value units, defined in Equation 2 as:

$$\text{N-value} = -100\log_{10}(I/F) \quad (2)$$

where  $I$  is the measured radiance and  $F$  is the TOA incoming solar flux.

The partial derivatives (Jacobians) on the right-hand side form a Jacobian  $K$ -matrix. The matrix consists of the  $N$  value sensitivities associated with linear perturbations in state vector parameters:  $\text{SO}_2$ ,  $\text{O}_3$  and  $dR/d\lambda$  (*i.e.*, reflectivity spectral slope)

$$K = \begin{pmatrix} \frac{\partial N_{317}}{\partial \text{SO}_2} & \frac{\partial N_{317}}{\partial \text{O}_3} & \frac{\partial N_{317}}{\partial x} (\lambda_i - \lambda_R) \\ \frac{\partial N_{331}}{\partial \text{SO}_2} & \frac{\partial N_{331}}{\partial \text{O}_3} & \frac{\partial N_{331}}{\partial R} (\lambda_i - \lambda_R) \\ \frac{\partial N_{340}}{\partial \text{SO}_2} & \frac{\partial N_{340}}{\partial \text{O}_3} & \frac{\partial N_{340}}{\partial R} (\lambda_i - \lambda_R) \end{pmatrix} \quad (3)$$

The  $K$  matrix elements are computed as finite differences for each retrieved parameter and each spectral band from the pre-computed BUV radiance look-up tables (LUT). The LUT's nodal points correspond to surface pressure, satellite-viewing geometry (solar zenith, satellite nadir, and relative azimuthal angles), total ozone and column  $\text{SO}_2$ , assuming TOMS standard Ozone profiles. For  $\text{SO}_2$  the algorithm assumes three Gaussian shape profiles (2-km half-width), with different

peak SO<sub>2</sub> altitudes: 8 km (middle troposphere, TRM data), 13 km (upper troposphere, TRU data), and 18 km (lower stratosphere, STL data). The radiative transfer (RT) calculations were computed off-line using TOMRAD radiative transfer code (Dave 1965).

The state vector increment,  $\Delta \mathbf{x}$ , is defined in (4). The adjustment to  $\Delta \mathbf{x}$  after each iteration is subsequently determined by inverting the 3 x 3 Jacobian matrix  $\mathbf{K}$ :

$$\Delta \mathbf{x} = \mathbf{K}^{-1} \Delta \mathbf{y} = \begin{pmatrix} \Delta SO_2 \\ \Delta O_3 \\ \Delta \frac{\partial R}{\partial \lambda} \end{pmatrix} \quad (4)$$

The differentials  $\Delta \mathbf{x}$  are added to the previous iteration state  $\mathbf{x}$  values, beginning with a first guess to obtain the column amounts of SO<sub>2</sub> and O<sub>3</sub> in Dobson units (1 DU= 2.69\*10<sup>16</sup> molec·cm<sup>-2</sup>) and  $\partial R/\partial \lambda$  [nm<sup>-1</sup>]. The largest change in SO<sub>2</sub> column amount occurs in the first iteration and the process typically converges in 2-3 iterations depending on the actual SO<sub>2</sub> amount.

### 2.3 Step 2 Retrieval

The MS\_SO2 forward model accounts for O<sub>3</sub> ( $\Omega$ ) and SO<sub>2</sub> ( $\Sigma$ ) absorption and linear spectral changes in R due to the mixing of aerosols in the SO<sub>2</sub> plume. The algorithm, however, does not explicitly characterize the absorption and non-

linear scattering effects of volcanic ash (absorbing) and sulfate (non-absorbing) aerosols. The retrieval errors in  $\Sigma$  and  $\Omega$  caused by volcanic ash during the first days after an explosive eruption can be significant in the case of major volcanic eruptions like Pinatubo and El Chichon (Krueger et al., 1995; Krotkov et al., 1997). A step 2 procedure was developed to handle explosive eruptions (VEI > 3), in which large  $\Omega$  anomalies have a propensity to occur in conjunction with high ash concentrations. In step 2, a corrected total ozone  $\Omega_{\text{cor}}$  inside the SO<sub>2</sub> cloud is constrained using the retrieved  $\Omega$  outside the plume along the orbit for each cross-track position. The step 2 part of the algorithm was substantially improved in this release (v2). Changes to the algorithm include a modified FOV selection criterion and a better method of interpolating the ozone inside the SO<sub>2</sub> plume.

### *2.3.1 FOV Selection Criterium*

In deciding whether to apply Step 2, the algorithm considers  $\Sigma$ ,  $\Omega$  and aerosol index (AI) retrieved in Step 1. The AI is estimated from retrieved and forward model generated parameters as shown in Eq. (5):

$$AI = \frac{\partial N_{340}}{\partial R} \frac{\partial R}{\partial \lambda} (\lambda_{340} - \lambda_{380}) = -40 \cdot \frac{\partial N_{340}}{\partial R} \frac{\partial R}{\partial \lambda}, \quad (5)$$

where  $\partial R/\partial \lambda$  characterizes the spectral reflectivity dependence and  $\partial N/\partial R$  represents the Jacobian with respect to R retrieved at 340 nm. The AI can be qualitatively used to identify spatial regions affected by absorbing aerosols (dust, smoke, ash). The step 2 selection criterion first identifies FoVs for which either

$\text{SO}_2 > 15$  DU (inside the plume) or  $\text{AI} > 6$  (implying high absorbing aerosols concentrations). The additional AI criterium allows for the selection of FoVs around the edges of the cloud, where the  $\text{SO}_2$  can be underestimated due to high aerosol concentrations. In this case, it is assumed that the step 1  $\text{SO}_2$  may have been underestimated due to the ozone error caused by ash absorption. In these cases, the  $\text{SO}_2$  error can cause the retrieved  $\text{SO}_2$  to be less than 15 DU threshold applied in calculating  $\text{SO}_2$  burdens from volcanic sources. The resulting sample of FOVs characterizes the  $\text{SO}_2$  cloud region. Each FOV in this sample is then tested to determine whether a second retrieval is performed, depending on whether either  $\Omega_{\text{step1}} > \bar{O}_3 + \sigma_{O_3}$  or  $\text{AI} > 1.5$  is true. Here  $\bar{O}_3$  represents the regional mean ozone outside the plume and  $\sigma_{O_3}$  represents the standard deviation in the regional mean.

A second retrieval is performed on the FOVs satisfying either selection criterium. The most important step in this process is the ozone correction because this correction directly affects the  $\text{SO}_2$  retrieved in step 2. The ozone is corrected by masking the volcanic plume region and then linearly interpolating  $\text{O}_3$  outside the plume, along the orbital track for each affected swath position.

### *2.3.2 Interpolation methodology*

The new interpolation scheme is performed piecewise, for the regions above (north) and below (south) of the selected pixel. Ozone values inside the plume area

are excluded from the interpolation. Ozone values exceeding the highest nodal point in the ozone table (e.g., tropical, mid-latitude, and high latitude) are also excluded. The interpolation is performed along the orbital track of the satellite and is confined to a latitudinal range 30° north and south of the target FoV.

Two linear regressions are then performed on each of the two latitudinal subsamples, resulting in two sets of regression parameters north and south of the target FoV. These parameters are used in Eq. (6a) and Eq. (6b) to obtain two values,  $\Omega_1$  and  $\Omega_2$ , at the position of the target pixel,  $\varphi_{\Omega 0}$ :

$$\Omega_1 = m_1 \varphi_{\Omega 0} + b_1 \quad (6a)$$

$$\Omega_2 = m_2 \varphi_{\Omega 0} + b_2 \quad (6b)$$

A corrected ozone is computed by weighting  $\Omega_1$  and  $\Omega_2$  by the relative distance of the target pixel to the plume's south and north boundaries,  $d_1$  and  $d_2$ , as shown in Eq (7a) and Eq (7b):

$$w_1 = \frac{d_1}{d_1 + d_2} \quad (7a)$$

$$w_2 = \frac{d_2}{d_1 + d_2}. \quad (7b)$$

The corrected ozone value,  $\Omega_{cor}$ , is subsequently determined by computing a distance weighted ozone as shown in Eq. (8),

$$\Omega_{cor} = w_1 \Omega_1 + w_2 \Omega_2. \quad (8)$$

A modified retrieval is then performed on the selected pixels using a 2 x 2 K-matrix that only includes the radiances at 317 and 340 nm. Note that even though the corrected O<sub>3</sub> is not explicitly used in the construction of the K-matrix, it places a fixed constraint on the O<sub>3</sub> node in the LUTs. A step 2 algorithm flag is provided in the product. The flag informs users whether step 2 was applied and which of the above criteria was used in the selection process.

### *2.3.3 O<sub>3</sub> and SO<sub>2</sub> corrections*

The correction to step 1 SO<sub>2</sub> retrieval can be significant depending on the size of the O<sub>3</sub> anomaly. For illustration purposes, consider the case of El Chichon, which erupted on April 4, 1982. The step 1 and step 2 SO<sub>2</sub> and O<sub>3</sub> retrieved by TOMS are shown in Fig. 2. The AI is shown in Fig. 3. The SO<sub>2</sub> and O<sub>3</sub> errors due to the mixing of aerosols can be computed from the difference between step 1 and step 2 as shown in Fig. 4. As can be seen in Fig. 4, these errors are highly correlated and have a negative slope. Consequently, an increase in dO<sub>3</sub> due to ash absorption causes a decrease in dSO<sub>2</sub>. Since this version has better skill at estimating the corrected ozone, this leads to an improved retrieval of the SO<sub>2</sub> column.

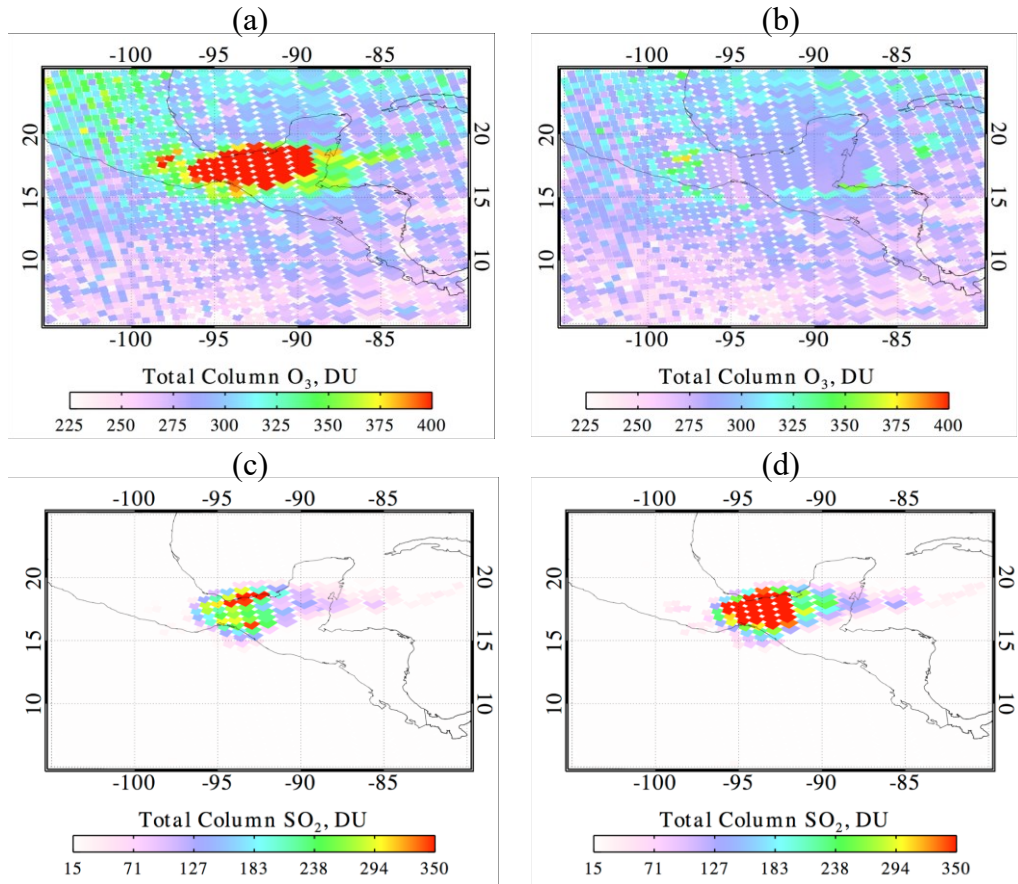


Figure 2. MS\_SO2 imagery showing a) Step 1 total column O<sub>3</sub>, b) Step 2 total column O<sub>3</sub> c) Step 1 total column SO<sub>2</sub> and d) Step 2 total column SO<sub>2</sub> from El Chichon eruption on April 4, 1982.

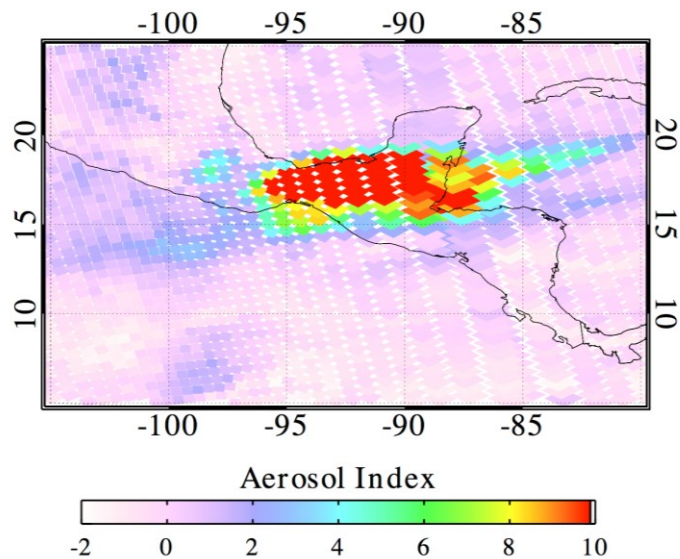


Figure 3. Aerosol Index for the El Chichon eruption on April 4, 1982, computed from retrieved  $\partial R/\partial \lambda$ .

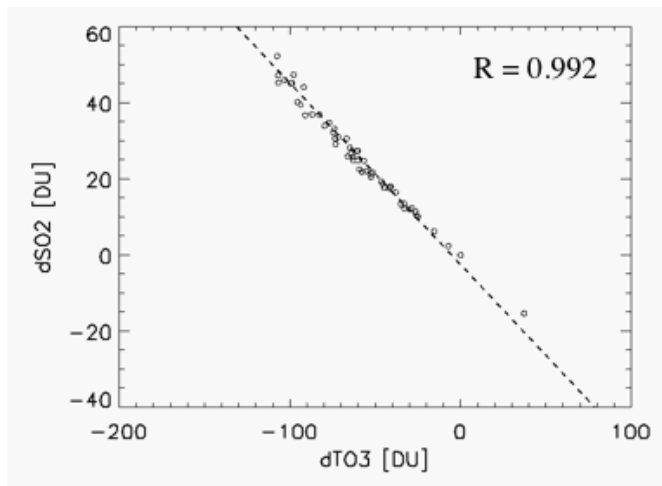


Figure 4. The differences between Step 2 and Step 1 ozone and SO<sub>2</sub> for the April 4 1982 El Chichon case shown in Figure 2. It can be seen that the O<sub>3</sub> errors are anti-correlated with SO<sub>2</sub> step 1 errors.

#### 2.4 Soft Calibration of the 340 Channel

The mean TOMS-retrieved SO<sub>2</sub> background far away from any SO<sub>2</sub> sources is assumed to be zero, but due to noise in the retrieval system (*e.g.*, instrument, forward and inversion models), the retrieved SO<sub>2</sub> values fluctuate around zero (positive and negative). To correct for any residual SO<sub>2</sub> bias in the mean background, the algorithm uses inversion of the K-matrix – what Rogers (2000) refers to as the gain matrix (or G-matrix) – and uses the matrix element associated with the SO<sub>2</sub> sensitivity at 340 nm to calibrate the 340 radiance.

An SO<sub>2</sub>- and aerosol-free TOMS orbit over the central Pacific was selected for this procedure. A Step 1 retrieval is then performed for this orbit with no soft calibration applied. Using the SO<sub>2</sub> field generated for this orbit, a correction to the 340 radiance is then computed as shown in (9)

$$dN_{340} = Mean\left(\frac{SO_2}{\frac{\partial SO_2}{\partial N_{340}}}\right) \quad (9)$$

where,  $\partial SO_2 / \partial N_{340}$  is the (2,2) G-matrix element corresponding to the SO<sub>2</sub> sensitivity in the 340 spectral band. Figure 5 shows a plot of the N-value correction applied to the 340 nm channel.

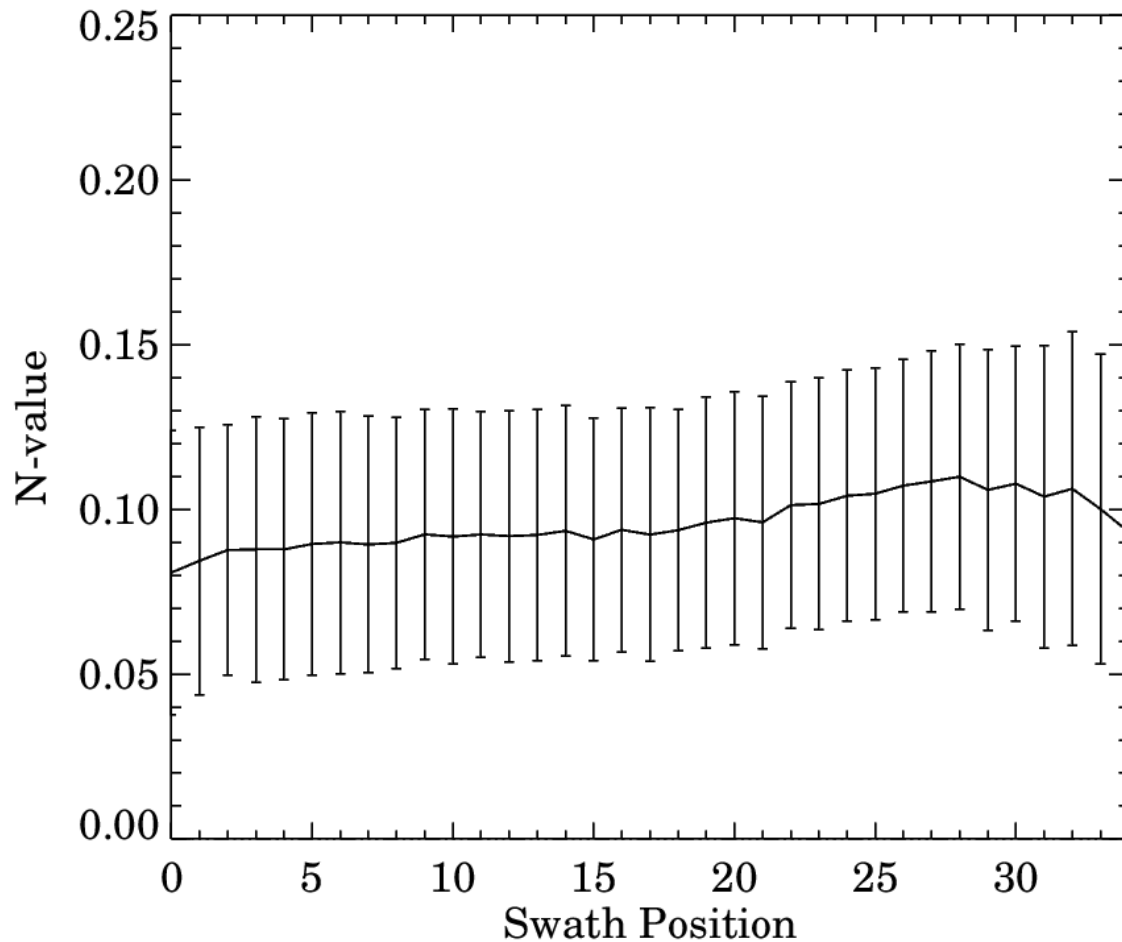


Figure 5. N-Value correction of the 340 nm channel as a function of the swath position. Error bars are also shown. A positive N-value correction results in a small reduction in the retrieved  $\text{SO}_2$

### *2.5 $\text{SO}_2$ retrieval noise*

The retrieval of volcanic  $\text{SO}_2$  is subject to limitations related to the sensitivity of the instrument and the skill of the forward model in simulating the UV radiances. Noise in the retrieval system produces a non-biased near-Gaussian distribution in the  $\text{SO}_2$  background values with zero expected value. We characterize the sensitivity of the instrument by estimating the standard deviation of the distribution of background  $\text{SO}_2$  retrieved in regions where  $\text{SO}_2$

concentrations are considered well below the detection limit of the TOMS instrument.

Figure 6 shows background SO<sub>2</sub> PDFs (6a) and standard deviations (6b) applying MS\_SO2 algorithm to the Nimbus 7 TOMS and the currently flying next generation hyperspectral Ozone Mapping Profiling Suite Nadir Mapper (OMPS-NM) on board the Suomi National Polar-orbiting Partnership (NPP) and NOAA 20 satellites. The random errors in the MS\_SO2 retrieval were estimated from the standard deviation in the SO<sub>2</sub> from a large data sample that included 90 central Pacific orbits, spanning a ten-year period between 1980 and 1990. For this comparison, we selected one month of NPP/OMPS spectral data (central Pacific) and applied the MS\_SO2 algorithm using the same four wavelength bands on TOMS (Table 2), which were first convolved with the TOMS bandpass function.

Data were restricted to  $\Sigma$  values between -20 and 20 DU (Fig. 6a). Standard deviations were then computed as a function of the TOMS or OMPS cross-track position as shown in Fig. 6b. Figure 6b can be used to characterize and compare the SO<sub>2</sub> detection limits for Nimbus-7 TOMS and OMPS applying the same MS\_SO2 retrieval algorithm using the same four TOMS wavelength bands (Table 2).

Figure 6b shows that TOMS retrieval noise depends on the swath position, varying from ~ 6 DU at nadir to ~4 DU at higher viewing angles, while OMPS

noise is 2-3 times smaller ( $\sim 2$  DU) and is relatively independent of the cross-track position (Figure 6b). Using the same MS\_SO2 algorithm, we subsequently estimate the SO<sub>2</sub> detection limit for TOMS and OMPS-NM to be about 15 DU and 6 DU ( $\sim 99\%$  confidence level), respectively. We set the TOMS sensitivity threshold for detecting volcanic SO<sub>2</sub> at 15 DU, just below the 99% confidence interval.

We note that applying the hyperspectral Principal Component Analysis (PCA) algorithm (Li et al., 2013) to all the 100-200 wavelengths available from the OMPS-NM hyperspectral measurements, the noise standard deviation is reduced by an order of magnitude to  $\sim 0.2-0.5$  DU, allowing detection of large anthropogenic point sources (emissions more than  $\sim 80$  kt yr<sup>-1</sup>) (Fioletov et al., 2016; Zhang et al., 2017).

The random error associated with the SO<sub>2</sub> retrieved inside volcanic clouds can be characterized by comparing two independent UV algorithms applied to the same BUV measurements (Figure 7). For several large volcanic cases, we compared MS\_SO2 retrievals with independent SO<sub>2</sub> retrievals from the Principal Components Analysis algorithm (PCA). For this comparison, the PCA algorithm has been modified to use all 6 TOMS spectral channels (normally it is applied to a hyper spectral instruments). The random error is estimated by computing the standard deviation in clean regions of the atmosphere. The random error provides a

measure of the sensitivity of the instrument. For SO<sub>2</sub> mass calculations, we apply an SO<sub>2</sub> threshold of 15 DU (about 2 to 3  $\sigma$  with respect to figure 6a).

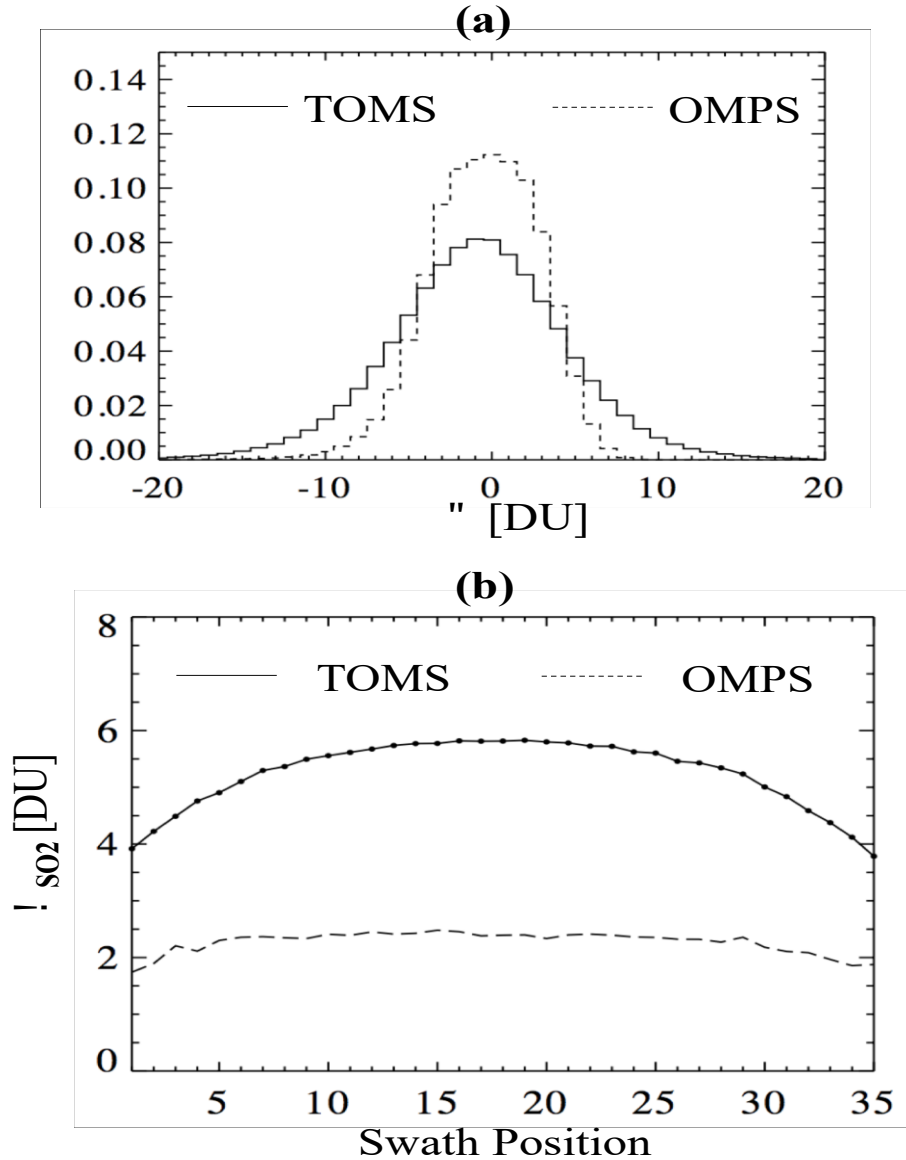


Figure 6. a) Noise PDF for background SO<sub>2</sub> retrievals applying the same MS\_SO2 algorithm to the Nimbus-7 TOMS and SNPP OMPS measurements b) the SO<sub>2</sub> retrieval noise standard deviation for TOMS (solid line) and OMPS (dashed line) as a function of the cross-track position. OMPS noise is a factor of 2-3 less compared to TOMS and less dependent on cross-track position.

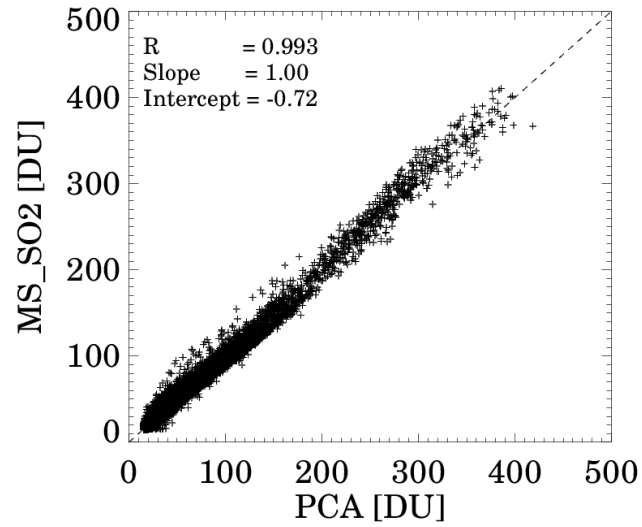


Figure 7. Scatterplot comparing volcanic SO<sub>2</sub> retrievals applying two independent MS\_SO2 and the PCA algorithms to the TOMS measurements for several major eruptions spanning the full dynamic range of the SO<sub>2</sub> retrievals.

### 3. DATASET ORGANIZATION

The TOMSN7SO2 product provides a set of Level 2 orbital swath files produced by applying the MS\_SO2 algorithm to the complete N7-TOMS data record.

#### *3.1 File Naming Convention*

The TOMSN7SO2 data granules (files) are named as in this example:

*TOMS-N7\_L2-TOMSN7SO2\_1991m0817t090821-o64696\_v03-00-2019m0607t165614.h5,*

where the components of filename are as follows:

1. Instrument (TOMS)
2. Spacecraft (N7)
3. Process Level (L2)
4. ESDT Short Name (TOMSN7SO2)
5. Date and Time at Start of Orbit (1991-08-17 09:08:21 UTC)
6. Orbit Number (64696)
7. Product Version (03-00)
8. Production Date and Time (2019-06-07 16:56:14 UTC)
9. File Type (h5)

#### *3.2 File Format and Structure*

The TOMSN7SO2 data granules are in plain HDF5 that is netCDF4-compatible and CF-compliant. Each TOMSN7SO2 data granule contains global attributes, dimensions, an ancillary data group, a geolocation data group, a science data group, and a sensor data group.

### *3.3 Key Science Data Fields*

The TOMSN7SO2 science product provides four key science data fields associated with the retrieval: SO<sub>2</sub> column amount, O<sub>3</sub> column amount, the Lambertian Equivalent Reflectivity at 380 nm (R), and the reflectivity spectral slope ( $\partial R/\partial \lambda$ ). The other retrieved parameters provide important diagnostic information.

#### *3.3.1 SO<sub>2</sub> Column Amount*

ColumnAmountSO2\_TRM, ColumnAmountSO2\_TRU and ColumnAmountSO2\_STL are, respectively, the column amounts for SO<sub>2</sub> in assumed Gaussian vertical distributions with 2-km standard deviations centered in the middle troposphere (8 km), the upper tropical troposphere (13 km) and the lower stratosphere (18 km).

#### *3.3.2 O<sub>3</sub> Column Amount*

ColumnAmountO3\_TRM, ColumnAmountO3\_TRU and ColumnAmountO3\_STL are, respectively, the O<sub>3</sub> total column amounts that

correspond to the SO<sub>2</sub> retrievals for the middle troposphere (8 km), the upper troposphere (13 km) and the lower stratosphere (18 km).

### *3.3.3 Lambertian Equivalent Reflectivity at 380 nm*

The FOV effective Lambertian Equivalent Reflectivity at 380 nm (LER380) models the combined surface, clouds and aerosols in TOMS FOV. It is independent of the ozone, SO<sub>2</sub> or height of the assumed SO<sub>2</sub> layer.

### *3.3.4 Reflectivity Spectral Dependence ( $\partial R/\partial \lambda$ )*

$dR/d\lambda_{TRM}$ ,  $dR/d\lambda_{TRU}$  and  $dR/d\lambda_{STL}$  are, respectively, the reflectivity spectral slopes ( $\partial R/\partial \lambda$ ), which represent the combined spectral dependence of surface, clouds and aerosols in TOMS FOV. They correspond to the SO<sub>2</sub> retrievals for the middle troposphere (8 km), the upper troposphere (13 km) and the lower stratosphere (18 km).

## 4. DATA CONTENTS

Each TOMSN7SO<sub>2</sub> data granule contains global attributes, dimensions, an ancillary data group, a geolocation data group, a science data group, and a sensor

data group. This section provides specific details regarding these components, as shown in Figure 8.

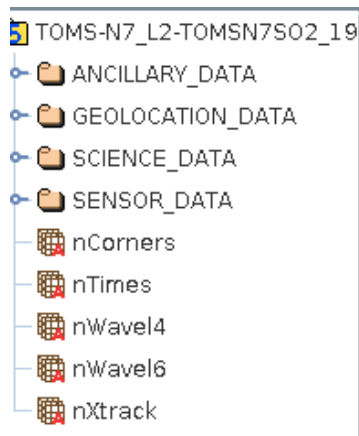


Figure 8. Shows 4 main data groups and dimensions.

#### *4.1 Global Attributes*

There are 43 global attributes in each TOMSN7SO2 data granule as shown in Figure 9.

```
Number of attributes = 43
AuthorAffiliation = NASA/GSFC
AuthorName = N. Krotkov, et al.
Conventions = CF-1.6
DataSetQuality = Under investigation.
DayNightFlag = Day
EastBoundingCoordinate = 180.0
EquatorCrossingDate = 1991-08-17
EquatorCrossingLongitude = 13.719999
EquatorCrossingTime = 10:00:26
FOVResolution = 50x50km
GranuleDayOfMonth = 17
GranuleDayOfYear = 229
GranuleMonth = 8
GranuleYear = 1991
HDFVersion = 5-1.8.12
InputPointer = TOMS-N7_L2-N7T03_1991m0817t0937-o64696_v001-2015m0910t025628.he5
InstrumentShortName = TOMS
LocalGranuleID = TOMS-N7_L2-TOMSN7SO2_1991m0817t090821-o64696_v03-00-2019m0607t165614.h5
LocalityValue = Global
LongName = TOMS/N7 MS SO2 Vertical Column 1-Orbit L2 Swath 50x50 km
NorthBoundingCoordinate = 89.74238
NumTimes = 392
OrbitNumber = 64696
PGEVersion = 1.1.4
ParameterName = Vertical Column Sulfur Dioxide
PlatformShortName = Nimbus 7
ProcessLevel = 2
ProcessingCenter = ACPS
ProductType = L2 Swath
ProductionDateTime = 2019-06-07T16:56:14.0Z
RangeBeginningDate = 1991-08-17
RangeBeginningTime = 09:08:21
RangeEndingDate = 1991-08-17
RangeEndingTime = 10:52:29
SensorShortName = Single Monochromator
ShortName = TOMSN7SO2
Source = N7/TOMS
SouthBoundingCoordinate = -78.02539
TAI93At0zOfGranule = -4.3459201E7
VersionID = 3
WestBoundingCoordinate = -180.0
identifier_product_doi = 10.5067/MEASURES/SO2/DATA204
identifier_product_doi_authority = http://dx.doi.org/
```

Figure 9. TOMSN7SO2 Global attributes

## 4.2 Dimensions

There are six dimensions in each TOMSN7SO2 data granule (Figure 5):

nCorners - The dimension representing the four ground-pixel corners of the TOMS FOV.

nTimes - The dimension representing the time of observation.

nWavel4 - The dimension representing the subset of four TOMS wavelengths used in the retrievals, i.e. 317,331,340 and 380.

nWavel6 - The dimension representing all six TOMS wavelengths.

nXtrack - The dimension representing the 35 cross-track scan positions.

### 4.3 Data Fields

#### 4.3.1 Ancillary Data

There are only two fields, CloudPressure and TerrainPressure, in the ancillary data group in each TOMSN7SO2 data.

#### 4.3.2 Geolocation Data

There are ten fields in the geolocation data group in each TOMSN7SO2 data granule as shown in Figure 10.

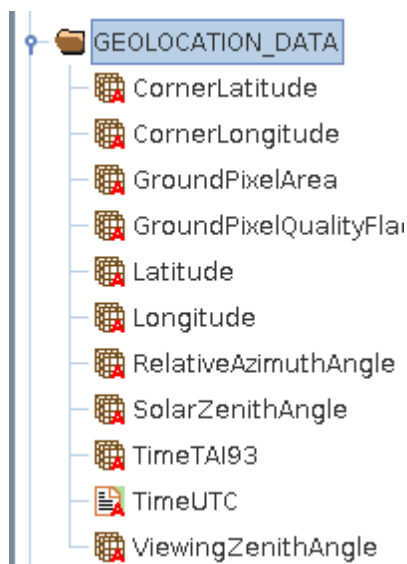


Figure 10. Geolocation Data Group

### 4.3.3 Science Data

There are 27 fields in the science data group in each TOMSN7SO2 data granule as shown in Figure 11.

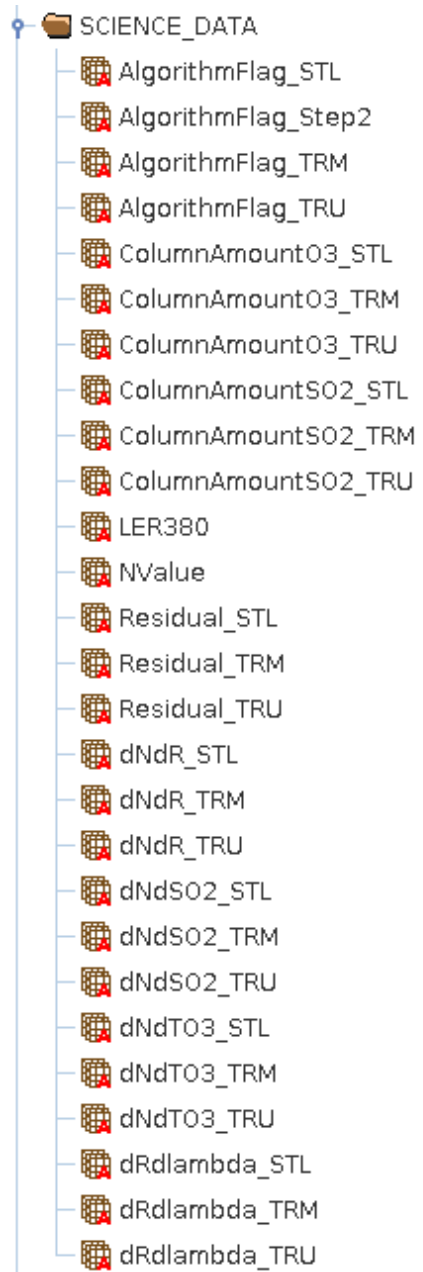


Figure 11. Science Data Group

#### 4.3.4 Sensor Data

There is only one field, Wavelength, in the sensor data group in each TOMSN7SO2 data granule. This field contains a list of the six TOMS wavelengths (312.34, 317.35, 331.06, 339.66, 359.88 and 379.95).

## 5. CONTACTS

Principal Investigator: Nickolay Krotkov  
[Nickolay.A.Krotkov@nasa.gov](mailto:Nickolay.A.Krotkov@nasa.gov)  
301-6114-5553

Algorithm Developer: Brad Fisher  
[bradford.fisher@ssaihq.com](mailto:bradford.fisher@ssaihq.com)  
301-867-2188

Algorithm Support: Peter Leonard  
[peter.j.leonard@nasa.gov](mailto:peter.j.leonard@nasa.gov)

## 6. DATA CITATION

### To cite the data in publications:

Nickolay A. Krotkov, Pawan K. Bhartia, Bradford Fisher, Peter Leonard (2017), TOMS/N7 MS SO2 Vertical Column 1-Orbit L2 Swath 50x50 km V2.00, Greenbelt, MD, USA, Goddard Earth Sciences Data and Information Services Center (GES DISC), Accessed: [*Data Access Date*], [10.5067/MEASURES/SO2/DATA202](https://doi.org/10.5067/MEASURES/SO2/DATA202)

## 6. REFERENCES

- Carn, S.A., Krueger, A.J., Bluth, G.J.S., Schaefer, S.J., Krotkov, N.A., Watson, I.M. and Datta, S. (2003), Volcanic eruption detection by the Total Ozone Mapping Spectrometer (TOMS) instruments: a 22-year record of sulfur dioxide and ash emissions, In: *Volcanic Degassing* (eds. C. Oppenheimer, D.M. Pyle and J. Barclay), *Geological Society, London, Special Publications*, **213**, pp.177-202.
- Dave, J. V., and C. L. Mateer, A preliminary study on the possibility of estimating total atmospheric ozone from satellite measurements, *J. Atm. Sci.*, 24, 414–427, 1967.
- Fisher, B. L., Krotkov, N. A., Bhartia, P. K., Li, C., Carn, S., Hughes, E., and Leonard, P. J. T. (2019), A new discrete wavelength UV algorithm for consistent volcanic SO<sub>2</sub> retrievals from multiple satellite missions, *Atmos. Meas. Tech. Discuss.*, doi:[10.5194/amt-2019-150](https://doi.org/10.5194/amt-2019-150), 2019.
- Heath, D.F., A.J. Krueger, H.A. Roeder, and B.D. Henderson, The Solar Backscatter Ultraviolet and Total Ozone Mapping Spectrometer (SBUV/TOMS) for Nimbus G, *Optical Engineering*, 14, 323, 1975
- Krotkov, N. A., A. J. Krueger, P. K. Bhartia, Ultraviolet optical model of volcanic clouds for remote sensing of ash and sulfur dioxide, *J. Geophys. Res.*, 102(D18), 21891-21904, 10.1029/97JD01690, 1997
- Krueger, A.J., Sighting of El Chichón sulfur dioxide clouds with the Nimbus 7 Total Ozone Mapping Spectrometer, *Science*, 220, p. 1377-1378, 1983.
- Krueger, A.J., L.S. Walter, P.K. Bhartia, C.C. Schnetzler, N.A. Krotkov, I. Sprod, and G.J.S. Bluth, Volcanic sulfur dioxide measurements from the Total Ozone Mapping Spectrometer (TOMS) Instruments, *Journal of Geophysical Research*, 100, D7, 14,057 - 14,076, 1995.
- Krueger, A. J., S. J. Schaefer, N. Krotkov, G. Bluth, and S. Barker, Ultraviolet remote sensing of volcanic emissions, in *Remote Sensing of Active Volcanism*, *Geophys. Monogr. Ser.*, vol. 116, edited by P. J. Mouginiis-Mark, J. A. Crisp, and J. H. Fink, pp. 25-43, AGU, Washington, D. C., 2000.
- Li, C., Krotkov, N. A., Carn, S., Zhang, Y., Spurr, R. J. D., and Joiner, J.: New-generation NASA Aura Ozone Monitoring Instrument (OMI) volcanic SO<sub>2</sub> dataset: Algorithm description, initial results, and continuation with the Suomi-NPP Ozone Mapping and Profiler Suite (OMPS), *Atmos. Meas. Tech.*, 10, 445-458, doi:[10.5194/amt-10-445-2017](https://doi.org/10.5194/amt-10-445-2017), 2017.
- McPeters, et al., Nimbus-7 Total Ozone Mapping Spectrometer (TOMS) data products user's guide, NASA Reference Publication 1384, pp1-67, 1996